INDONESIAN JOURNAL OF LIFE SCIENCES

Volume 5, No. 1, March 2023

RESEARCH ARTICLE

Artificial Intelligence Based Brain Tumor Localization Using YOLOv5

Muammar Sadrawi[1]*, Daniel Ryan Fugaha[1], Devita Mayanda Heerlie[1], Juan Lorell[1], Nicolaas Raditya Putra Gautama[1], Mohamad Zafran Aminuddin[1]

[1]Department of Bioinformatics, Institut Bio Scientia Internasional Indonesia, Jakarta, Indonesia

**corresponding author: muammar.sadrawi@i3l.ac.id*

A B S T R A C T

Brain tumors are caused by mutations in brain cells which cause them to divide uncontrollably. This disease has relatively low survival rate. Therefore, the earlier the tumor detected, the higher survival rate for the patient. This study develops the brain tumor detection system by utilizing the you only look once (YOLO). The model is based on YOLOv5 architect. The open dataset of tumorous images is utilized. From this dataset, the corresponding masks are given alongside the magnetic resonance imaging (MRI) dataset. Our study compares several YOLOv5 models to localize the brain tumor. The results show YOLOv5m (medium-sized), YOLOv5l (large-sized), and YOLOv5x (extra-large-sized) models have higher precision and recall values. The inference time from these models is relatively small for recent computational resources. In conclusion, the YOLOv5 models have produced superior result in localizing the brain tumor.

K E Y W O R D S

Brain Tumor Detection; Artificial Intelligence; YOLOv5

H I G H L I G H T S

- Brain tumor is a life-threatening event.
- Rapid and accurate detection will be significant.
- Artificial intelligence (AI) system is applied based on magnetic resonance imaging (MRI).
- Several YOLOv5 models are investigated.

INTRODUCTION

Brain related tumor or cancer has an incidence of more than 20,000 patients per year in United States (Cagney et al., 2017). It is an abnormal cell mass or growth in the brain with multiple types (Bian et al., 2018). The different types are benign (non-cancerous) and malignant (cancerous) brain tumors (Patel, 2020). The primary differences between the two is that benign tumors grow slower, have distinct borders, does not invade surrounding tissue or other parts of the body, whereas malignant tumors grow quickly and has irregular borders, along with invading surrounding tissue and also spreads to other parts of the body through metastasis (Ostrom et al., 2019; Vargo, 2017). Tumors are also graded from stage I to IV, with stage IV being the hardest to treat for an individual (McNeill, 2016).

The primary impact of brain tumor regardless of type could lead to fatality, which is due to the tumor compressing the brain in an enclosed space in the skull, thus leading to intracranial pressure (Devunooru et al., 2021). This compression is very damaging to the neural tissue due to the obstruction of cerebrospinal

fluid and increased swelling inside the cranial cavity which is responsible for many symptoms (Maschio, 2012; Richter et al., 2015). Therefore, an accurate early detection is indispensable.

Imaging system has been the golden standard for medical diagnostics. Echocardiography - Doppler based imaging – has been widely used for mitral regurgitation (Blumlein et al., 1986; Boltwood et al., 1983) and gallbladder (Bortoff et al., 2000). Meanwhile, another imaging technique - chest X-ray - is also regularly utilized in order to evaluate cardiomegaly by investigating the cardio to thorax ratio (Alghamdi et al., 2020). Another advanced technique, magnetic resonance imaging (MRI), is also deployed for several diseases detections such as chronic kidney disease (CKD) (Selby et al., 2018), Parkinson, (Heim et al., 2017) and cardiomyopathy (Rickers et al., 2005).

On the other hand, artificial intelligence (AI) has been advancing rapidly in pattern recognition for signal and image-based input systems. For signal processing, it was used for hemodynamics system (Sadrawi et al., 2021). In this study, the convolutional autoencoder was utilized to generate cardiovascular and cerebral hemodynamics signals. An AI system was also utilized to detect Parkinson disease by using electroencephalography –brain signal (Oh et al., 2020). This convolutional neural network (CNN) based model produced well sensitivity and specificity in identifying either the subject has Parkinson disease.

More specifically, AI has yielded astonishing consequences for image-based input systems. The CNN based system was deployed for distinguishing benign and malignant skin lesions for the skin cancer detection framework (Esteva et al., 2017). A seven-layer CNN was also applied for periodontal bone loss detection (Krois et al., 2019). This previous study utilized the dental radiography images. Another study used CNN based Darknet-19 YOLO modified system to differentiate between COVID-19, pneumonia, and clear lung conditions (Ozturk et al., 2020). This related research used 17 convolution layer CNN model and chest X-ray images. Interestingly, AI based imaging diagnostics research has also been conducted for brain tumors (El-Dahshan et al., 2014; Noreen et al., 2020).

Particularly for YOLOv5 system, it has been widely used in many fields. It was used for plant related disease detection system (Chen et al., 2022). It was also utilized for investigating the fruit quality (Yao et al., 2021). Further, YOLOv5 based system was deployed for fruit-picking robot (Yan et al., 2021). In recent years, the modified YOLOv5 was operated for the vehicle system (Zhang et al., 2022). As it can be seen, there are extensive disciplines have involved the YOLOv5 based system.

As aforementioned information, this study has a purpose of developing an AI based brain tumor detection system. The system is based on YOLOv5 (Jocher et al., 2020). The structure of this study is the introduction, material and methods, result and discussion, and conclusion.

MATERIAL AND METHODS

The data used in this study is based on a dataset (Cheng et al., 2015; Cheng et al., 2016; Cheng, 2017). It was used to gather the Brain MRI images for the brain tumor detection dataset. The images in this dataset are divided into two categories: healthy brains and detected brain tumors. This study utilized 200 tumorous MRI images. Image size 640 x 640 pixels.

Normally, the object detection system utilizes the CNN model. For YOLOv5, it contains three main parts: backbone, neck and head. The backbone applies the Cross Stage Partial Network (CSPNet). The neck utilizes Path Aggregation Network (PANet) and the YOLO is deployed for the head for the classifier and regressor.

The flowchart of study is given in Figure 1. Initially from the raw data, this dataset is divided for the training and testing without any overlapping. The YOLOv5 models are prepared for the training system. The trained weight later is evaluated using the testing data. This will generate the estimated classes and the bounding boxes.

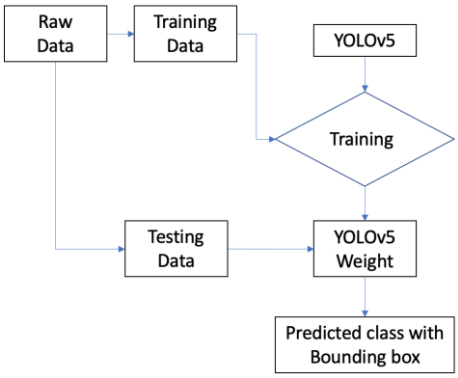

Figure 1. Flowchart of study

For the coding, Python 3.8.10, PyTorch v1.13.1 and CUDA 11.6 are utilized. For the hyperparameter is given in Table 1. This study compares different YOLO models - YOLOv5n (nano), YOLOv5s (small), YOLOv5m (medium), YOLOv5l (large), YOLOv5x (extra-large). Further, we also consider the model size and the quality of prediction. In this system, for the training optimizer, we utilize stochastic gradient descend (Amari et al., 1993). This optimizer has been well utilized by prior studies (Hong et al., 2023; Yang et al., 2018).

Table 1. Training hyperparameter.

Parameter	Value
Optimizer	Stochastic Gradient Descend (SGD)
Learning rate	0.01
Epoch	20
Batch size	16

Table 2. Confusion Matrix.

		Actual	
		Tumor	**Normal**
Prediction	**Tumor**	TP	FP
	Normal	FN	TN

$$Precision = TP/(TP + FP) \quad (1)$$

$$Recall = TP/(TP + FN) \quad (2)$$

Here, TP is the true positive, FN is the false negative, and FP is the false positive. The precision is the ratio between the TP and all positive classes, shown in Eq. 1. Meanwhile, recall is the ratio between the TP and summation of TP and FN, given in Eq. 2. For all evaluation is given in confusion matrix in Table 2. In order to define this parameter, the threshold for the intersection over union (IoU) is defined as 0.5. The IoU is to quantify the overlap between the predicted bounding box and the ground truth.

RESULTS AND DISCUSSION

This study utilizes several YOLOv5 models to localize the tumorous part in brain. It uses several brain images with its corresponding masks. The input of the is 640 x 640 pixels. The output of the YOLOv5 model

is the detected classes with its bounding boxes: X center, Y center, width and height. The given output also provides the probability from a detected class. The evaluations are based on the bounding box loss, objectness loss, precision, recall, and mean average precisions. Further, the investigation of the inference time is also conducted to investigate the estimation time for prediction.

Figure 2 shows the model convergence during training session. It can be seen for the bounding box loss, the YOLOv5l, YOLOv5m, and YOLOv5x converged better by producing lower mean squared error (MSE) than YOLOv5n and YOLOv5s. Furthermore, those models are relatively less oscillated, given in Figure 2(a). Meanwhile, Figure 2(b) produces parallel result to Figure 2(a) for the objectness loss. In this system, initially the models YOLOv5n and YOLOv5s reduce earlier, however the models YOLOv5l, YOLOv5m, and YOLOv5x consistently keep the slope of the convergence.

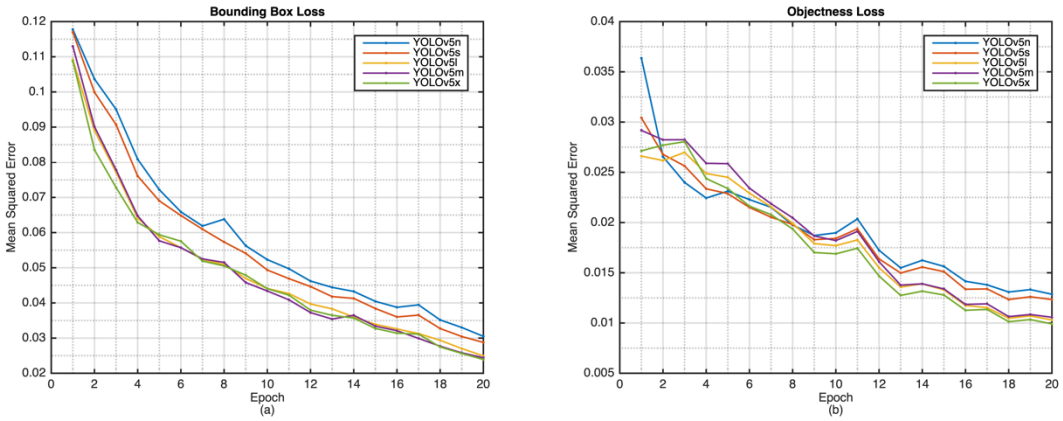

Figure 2. Training convergence. (a) Bounding Box Loss; (b) Objectness Loss.

The validation session is also similar to the training, shown in Figure 3. The YOLOv5l, YOLOv5m, and YOLOv5x generate higher accuracy than YOLOv5n and YOLOv5s. However, the validation curves are slightly fluctuated for the bounding box loss, given in Figure 3(a). On the other hand, the Figure 3(b) has similar phenomena with training objectness loss given in Figure 2(b).

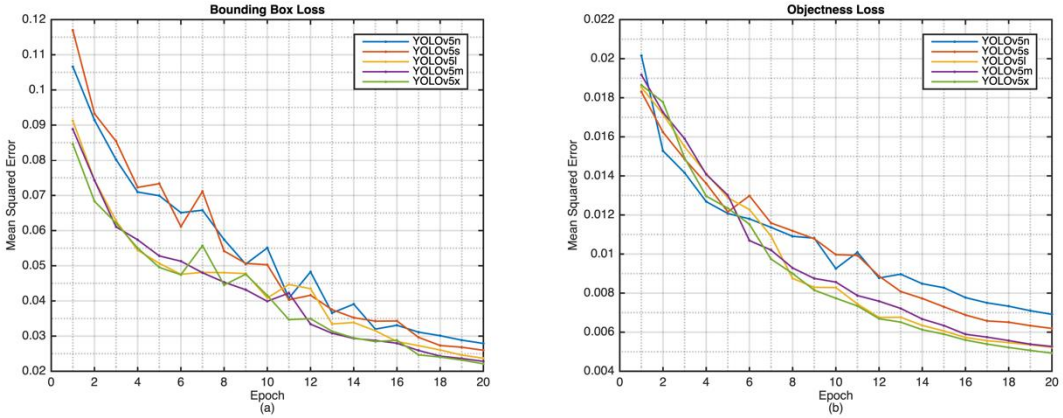

Figure 3. Validation convergence. (a) Bounding Box Loss; (b) Objectness Loss.

The fluctuation is relatively occurred in precision and recall, given in Figures 4(a) and 4(b). As it can be seen that the YOLOv5l, YOLOv5m, and YOLOv5x models have better results in those precision and recall matrix. For the mean average precision at threshold of 0.5 (mAP 0.5) and mean average precision at threshold of 0.5 to 0.95 (mAP 0.5:0.95), the YOLOv5l, YOLOv5m, and YOLOv5x models also generate higher values, shown in Figures 5(a) and 5(b). To investigate all model evaluation, it is given in Table 3. From this figure, the lower the loss the better. Oppositely, for the matrices, the higher value will produce the better

prediction.

Table 3. Model Evaluation

Models	Training Loss		Validation Loss		Metrices			
	Bounding Box	Objectness	Bounding Box	Objectness	Precision	Recall	mAP 0.5	mAP 0.5:0.95
YOLOv5n	0.030	0.013	0.028	0.007	0.898	0.884	0.926	0.630
YOLOv5s	0.029	0.012	0.026	0.006	0.919	0.929	0.947	0.661
YOLOv5m	0.025	0.010	0.024	0.005	0.972	0.965	0.976	0.711
YOLOv5l	0.024	0.011	0.023	0.005	0.954	0.960	0.973	0.726
YOLOv5x	0.024	0.01	0.022	0.005	0.969	0.985	0.973	0.726
Mean	**0.026**	**0.011**	**0.025**	**0.006**	**0.942**	**0.945**	**0.959**	**0.691**
Std	**0.003**	**0.001**	**0.002**	**0.001**	**0.033**	**0.039**	**0.022**	**0.043**

Note: The lower loss the better model; The higher matrices the better model

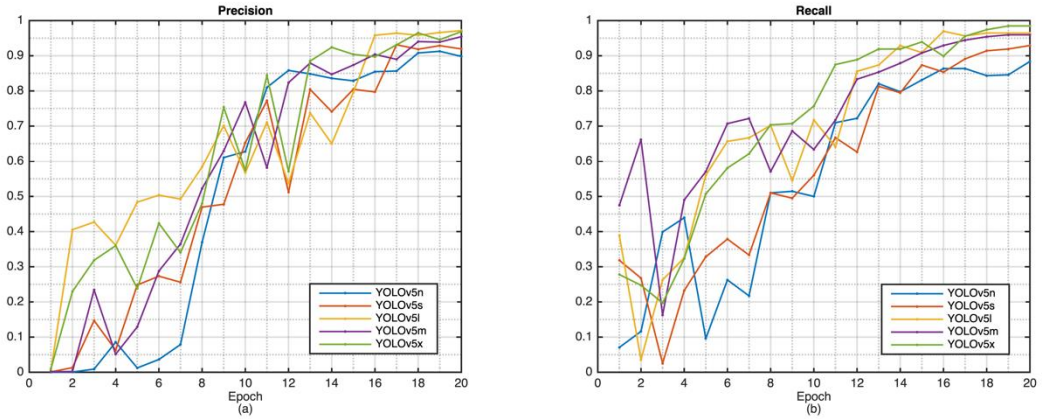

Figure 4. Matrix evaluation. (a) Precision; (b) Recall.

In order to investigate the predicted bounding boxes by the YOLOv5 models, this study randomly selected several tumorous images, given in Figure 6. In this figure, all YOLOv5 models were compared to the ground truth of tumor labelled masks.

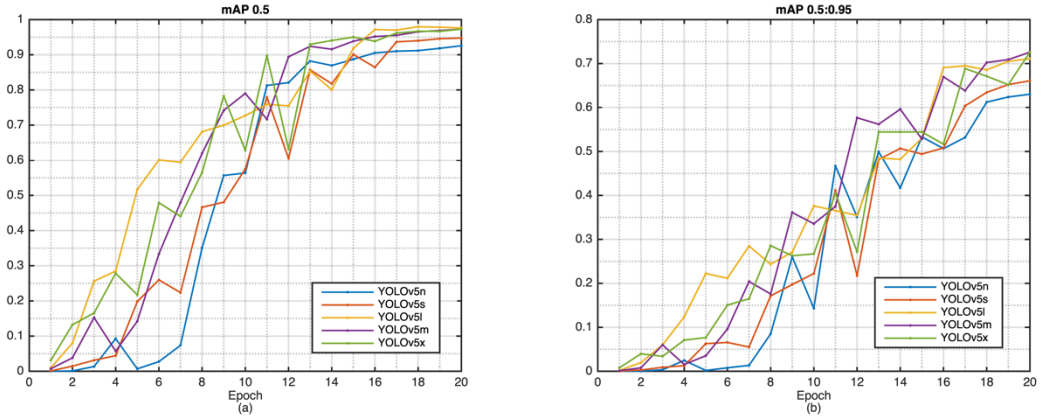

Figure 5. Mean Average Precision. (a) mAP 0.5; (b) mAP 0.5:0.95.

For evaluation of time related efficiency, the inference time for the model to perform the prediction must be investigated. From Table 4, it can be seen that the YOLOv5n has the shortest inference time compared to other models. It needs about 100 ms to perform the prediction. Meanwhile, the longest

inference time is generated by the YOLOv5x.

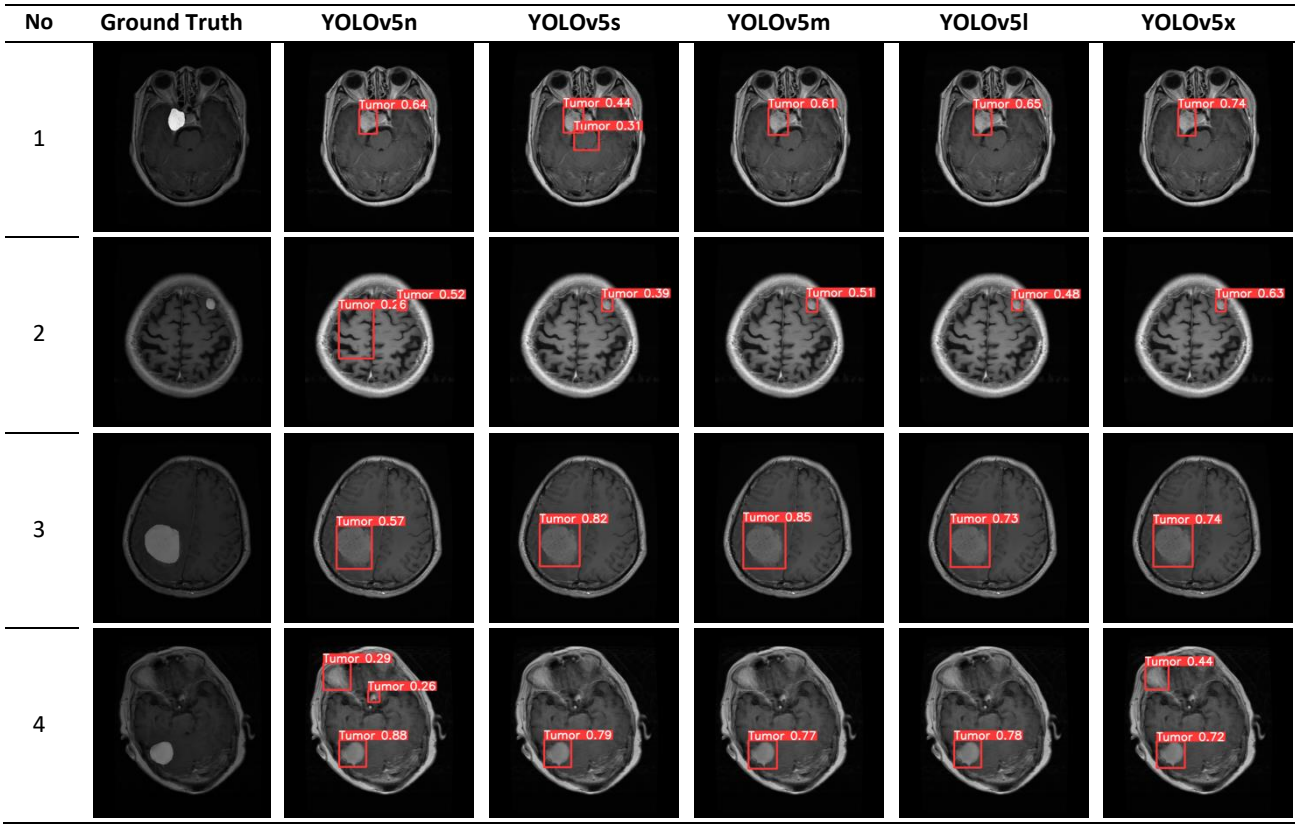

Figure 6. YOLOv5 model results.

Table 4. Inference Time YOLOv5 models [**Note**: The lower the better]

Model	Inference Time [ms]
YOLOv5n	125.2
YOLOv5s	363.7
YOLOv5m	956.4
YOLOv5l	1885.9
YOLOv5x	3443

For the benchmarking, several prior studies are utilized for the comparative study. An ensemble model was designed for the brain tumor detection by using MRI data (Ghafourian et al., 2023). This previous study used the voting system for naïve Bayes, support vector machine, and K nearest neighbor algorithms to distinguish between normal and tumorous images. The proposed method has an average accuracy of 98.61%, sensitivity of 95.79% and specificity of 99.71% in BRATS 2014 dataset. Furthermore, it has an average accuracy of 99.13%, sensitivity of 99% and specificity of 99.26% in BTD20 database. Another study utilized faster R CNN to segment the tumor (Bhanothu et al., 2020). This study used several hundreds of glioma, meningioma and pituitary tumors. This study has the average precision for glioma equals to 75.18%, meningioma for 89.45%, and pituitary for 68.18%. In overall it has mAP of 77.60%.

This study has some limitations. This study did not consider the stage of the tumor. The tumorous images utilized in this study are relatively obvious. Further, we did not specify the brain tumor classes as given in previous study (Bhanothu et al., 2020). This will likely be more challenging.

CONCLUSION

This study evaluates the possibility of implementation AI based system for brain detection. Six YOLOv5 models are compared to localize the tumor. It can be seen that most of the YOLOv5 models can be considered for the assistive system for the medical doctors in detecting brain tumor by evaluating the MRI data. Medically, the final option is definitely is based on the decision by the medical doctor.

REFERENCES

Alghamdi, S. S., Abdelaziz, I., Albadri, M., Alyanbaawi, S., Aljondi, R., & Tajaldeen, A. (2020). Study of cardiomegaly using chest x-ray. Journal of Radiation Research and Applied Sciences, 13(1), 460-467. https://doi.org/10.1080/16878507.2020.1756187

Amari, S. I. (1993). Backpropagation and stochastic gradient descent method. Neurocomputing, 5(4-5), 185-196. https://doi.org/10.1016/0925-2312(93)90006-O

Bhanothu, Y., Kamalakannan, A., & Rajamanickam, G. (2020, March). Detection and classification of brain tumor in MRI images using deep convolutional network. In 2020 6th international conference on advanced computing and communication systems (ICACCS) (pp. 248-252). IEEE.DOI: https://doi.org/10.1109/ICACCS48705.2020.9074375

Bian, S., Repic, M., Guo, Z., Kavirayani, A., Burkard, T., Bagley, J. A., Krauditsch, C., & Knoblich, J. A. (2018). Genetically engineered cerebral organoids model brain tumor formation. *Nature Methods*, *15*(8), 631–639. https://doi.org/10.1038/s41592-018-0070-7

Blumlein, S. A. N. M. B. T. E., Bouchard, A., Schiller, N. B., Dae, M., Byrd 3rd, B. F., Ports, T., & Botvinick, E. H. (1986). Quantitation of mitral regurgitation by Doppler echocardiography. Circulation, 74(2), 306-314. https://doi.org/10.1161/01.CIR.74.2.306

Boltwood, C. M., Tei, C., Wong, M. A. Y. L. E. N. E., & Shah, P. M. (1983). Quantitative echocardiography of the mitral complex in dilated cardiomyopathy: the mechanism of functional mitral regurgitation. Circulation, 68(3), 498-508. https://doi.org/10.1161/01.CIR.68.3.498

Bortoff, G. A., Chen, M. Y., Ott, D. J., Wolfman, N. T., & Routh, W. D. (2000). Gallbladder stones: imaging and intervention. *Radiographics*, *20*(3), 751-766. https://doi.org/10.1148/radiographics.20.3.g00ma16751

Cagney, D. N., Martin, A. M., Catalano, P. J., Redig, A. J., Lin, N. U., Lee, E. Q., ... & Aizer, A. A. (2017). Incidence and prognosis of patients with brain metastases at diagnosis of systemic malignancy: a population-based study. Neuro-oncology, 19(11), 1511-1521. https://doi.org/10.1093/neuonc/nox077

Chen, Z., Wu, R., Lin, Y., Li, C., Chen, S., Yuan, Z., ... & Zou, X. (2022). Plant disease recognition model based on improved YOLOv5. Agronomy, 12(2), 365. https://doi.org/10.3390/agronomy12020365

Cheng, J (2017). Brain tumor dataset. figshare. Dataset. https://doi.org/10.6084/m9.figshare.1512427.v5

Cheng, J., Huang, W., Cao, S., Yang, R., Yang, W., Yun, Z., ... & Feng, Q. (2015). Enhanced performance of brain tumor classification via tumor region augmentation and partition. PloS one, 10(10), e0140381. https://doi.org/10.1371/journal.pone.0140381

Cheng, J., Yang, W., Huang, M., Huang, W., Jiang, J., Zhou, Y., ... & Chen, W. (2016). Retrieval of brain tumors by adaptive spatial pooling and fisher vector representation. PloS one, 11(6), e0157112. https://doi.org/10.1371/journal.pone.0157112

Devunooru, S., Alsadoon, A., Chandana, P. W. C., & Beg, A. (2021). Deep learning neural networks for medical image segmentation of brain tumours for diagnosis: a recent review and taxonomy. *Journal of Ambient Intelligence and Humanized Computing*, *12*(1), 455-483. https://doi.org/10.1007/s12652-020-01998-w

Duran-Vega, M. A., Gonzalez-Mendoza, M., Chang-Fernandez, L., & Suarez-Ramirez, C. D. (2021). TYolov5: A Temporal Yolov5 Detector Based on Quasi-Recurrent Neural Networks for Real-Time Handgun Detection in Video. arXiv preprint arXiv:2111.08867. https://doi.org/10.48550/arXiv.2111.08867

El-Dahshan, E.-S. A., Mohsen, H. M., Revett, K., & Salem, A.-B. M. (2014). Computer-aided diagnosis of human brain tumor through MRI: A survey and a new algorithm. *Expert Systems with Applications*, *41*(11), 5526–5545. https://doi.org/10.1016/j.eswa.2014.01.021

Esteva, A., Kuprel, B., Novoa, R. A., Ko, J., Swetter, S. M., Blau, H. M., & Thrun, S. (2017). Dermatologist-level classification of skin cancer with deep neural networks. nature, 542(7639), 115-118. https://doi.org/10.1038/nature21056

Fradkov, A. L. (2020). Early history of machine learning. *IFAC-PapersOnLine*, *53*(2), 1385–1390. https://doi.org/10.1016/j.ifacol.2020.12.1888

Ghafourian, E., Samadifam, F., Fadavian, H., Jerfi Canatalay, P., Tajally A., Channumsin, S (2023). An Ensemble Model for the Diagnosis of Brain Tumors through MRIs. Diagnostics, 13(3):561. https://doi.org/10.3390/diagnostics13030561

Hamzenejadi, M. H., & Mohseni, H. (2022, November). Real-Time Vehicle Detection and Classification in UAV imagery Using Improved YOLOv5. In 2022 12th International Conference on Computer and Knowledge Engineering (ICCKE) (pp. 231-236). IEEE. https://doi.org/10.1109/ICCKE57176.2022.9960099

Heim, B., Krismer, F., De Marzi, R., & Seppi, K. (2017). Magnetic resonance imaging for the diagnosis of Parkinson's disease. Journal of neural transmission, 124(8), 915-964. https://doi.org/10.1007/s00702-017-1717-8

Hong, W., Ma, Z., Ye, B., Yu, G., Tang, T., Zheng, M (2023). Detection of Green Asparagus in Complex Environments Based on the Improved YOLOv5 Algorithm. Sensors, 23, 1562. https://doi.org/10.3390/s23031562

Hu, Y.-H. F., Ali, A., Hsieh, C.-C. G., & Williams, A. (2019). Machine learning techniques for classifying malicious API calls and N-Grams in Kaggle data-set. *2019 SoutheastCon*. https://doi.org/10.1109/SoutheastCon42311.2019.9020353

Krois, J., Ekert, T., Meinhold, L., Golla, T., Kharbot, B., Wittemeier, A., Dörfer, C. and Schwendicke, F., 2019. Deep learning for the radiographic detection of periodontal bone loss. Scientific reports, 9(1), pp.1-6. https://doi.org/10.1038/s41598-019-44839-3

Li, S., Li, Y., Li, Y., Li, M., & Xu, X. (2021). YOLO-FIRI: Improved YOLOv5 for Infrared Image Object Detection. IEEE Access, 9, 141861-141875. https://doi.org/10.1109/ACCESS.2021.3120870

Jung, H. K., & Choi, G. S. (2022). Improved yolov5: Efficient object detection using drone images under various conditions. Applied Sciences, 12(14), 7255. https://doi.org/10.3390/app12147255

Jocher, G. (2022, November 22). ultralytics/yolov5: v7.0 - YOLOv5 SOTA Realtime Instance Segmentation. Zenodo. https://doi.org/10.5281/zenodo.7347926

Maschio, M. (2012). Brain tumor-related epilepsy. *Current Neuropharmacology*, *10*(2), 124–133. https://doi.org/10.2174/157015912800604470

McNeill, K. A. (2016). Epidemiology of brain tumors. *Neurologic Clinics*, *34*(4), 981–998. https://doi.org/10.1016/j.ncl.2016.06.014

Noreen, N., Palaniappan, S., Qayyum, A., Ahmad, I., Imran, M., & Shoaib, M. (2020). A deep learning model based on concatenation approach for the diagnosis of brain tumor. *IEEE Access*, *8*, 55135–55144. https://doi.org/10.1109/access.2020.2978629

Oh, S. L., Hagiwara, Y., Raghavendra, U., Yuvaraj, R., Arunkumar, N., Murugappan, M., & Acharya, U. R. (2020). A deep learning approach for Parkinson's disease diagnosis from EEG signals. Neural Computing and Applications, 32(15), 10927-10933. https://doi.org/10.1007/s00521-018-3689-5

Ostrom, Q. T., Fahmideh, M. A., Cote, D. J., Muskens, I. S., Schraw, J. M., Scheurer, M. E., & Bondy, M. L. (2019). Risk factors for childhood and adult primary brain tumors. *Neuro-Oncology*, *21*(11), 1357–1375. https://doi.org/10.1093/neuonc/noz123

Ozturk, T., Talo, M., Yildirim, E. A., Baloglu, U. B., Yildirim, O., & Acharya, U. R. (2020). Automated detection of COVID-19 cases using deep neural networks with X-ray images. Computers in biology and medicine, 121, 103792. https://doi.org/10.1016/j.compbiomed.2020.103792

Patel, A. (2020). Benign vs malignant tumors. *JAMA Oncology*, *6*(9). https://doi.org/10.1001/jamaoncol.2020.2592

Richter, A., Woernle, C. M., Krayenbühl, N., Kollias, S., & Bellut, D. (2015). Affective symptoms and white matter changes in brain tumor patients. *World Neurosurgery*, *84*(4), 927–932. https://doi.org/10.1016/j.wneu.2015.05.031

Rickers, C., Wilke, N. M., Jerosch-Herold, M., Casey, S. A., Panse, P., Panse, N., ... & Maron, B. J. (2005). Utility of cardiac magnetic resonance imaging in the diagnosis of hypertrophic cardiomyopathy. Circulation, 112(6), 855-861. https://doi.org/10.1161/CIRCULATIONAHA.104.507723

Sadrawi, M., Lin, Y. T., Lin, C. H., Mathunjwa, B., Hsin, H. T., Fan, S. Z., ... & Shieh, J. S. (2021). Non-invasive hemodynamics monitoring system based on electrocardiography via deep convolutional autoencoder. Sensors, 21(18), 6264. https://doi.org/10.3390/s21186264

Selby, N. M., Blankestijn, P. J., Boor, P., Combe, C., Eckardt, K. U., Eikefjord, E., ... & Sourbron, S. (2018). Magnetic resonance imaging biomarkers for chronic kidney disease: a position paper from the European Cooperation in Science and Technology Action PARENCHIMA. Nephrology Dialysis Transplantation, 33(suppl_2), ii4-ii14. https://doi.org/10.1093/ndt/gfy152

Vargo, M. M. (2017). Brain tumors and metastases. *Physical Medicine and Rehabilitation Clinics of North America*, *28*(1), 115–141. https://doi.org/10.1016/j.pmr.2016.08.005

Yan, B., Fan, P., Lei, X., Liu, Z., & Yang, F. (2021). A real-time apple targets detection method for picking robot based on improved YOLOv5. Remote Sensing, 13(9), 1619. https://doi.org/10.3390/rs13091619

Yang, J., & Yang, G. (2018). Modified convolutional neural network based on dropout and the stochastic gradient descent optimizer. Algorithms, 11(3), 28. https://doi.org/10.3390/a11030028

Yao, J., Qi, J., Zhang, J., Shao, H., Yang, J., & Li, X. (2021). A real-time detection algorithm for Kiwifruit defects based on YOLOv5. Electronics, 10(14), 1711. https://doi.org/10.3390/electronics10141711

Zhang, Y., Guo, Z., Wu, J., Tian, Y., Tang, H., & Guo, X. (2022). Real-Time Vehicle Detection Based on Improved YOLO v5. Sustainability, 14(19), 12274. https://doi.org/10.3390/su141912274